Bioorganic & Medicinal Chemistry Letters 26 (2016) 1947–1953

Contents lists available at ScienceDirect

Bioorganic & Medicinal Chemistry Letters

journal homepage: www.elsevier.com/locate/bmcl

Development of thieno- and benzopyrimidinone inhibitors of the Hedgehog signaling pathway reveals PDE4-dependent and PDE4-independent mechanisms of action

Jonathan E. Hempel [a,b], Adrian G. Cadar [a,c], Charles C. Hong [a,b,d,*]

[a] Division of Cardiovascular Medicine, Vanderbilt University School of Medicine, 2220 Pierce Avenue, PRB 383, Nashville, TN 37232, USA
[b] Vanderbilt Institute of Chemical Biology, 896 Preston Research Building, Nashville, TN 37232, USA
[c] Department of Molecular Physiology and Biophysics, Vanderbilt University School of Medicine, 702 Light Hall, Nashville, TN 37232, USA
[d] Research Medicine, Veterans Affairs Tennessee Valley Healthcare System, Nashville, TN 37212, USA

ARTICLE INFO

Article history:
Received 21 January 2016
Revised 4 March 2016
Accepted 5 March 2016
Available online 7 March 2016

Keywords:
Hedgehog signaling pathway
Eggmanone
Suppressor of Fused
Phenotypic screening
Probe development

ABSTRACT

From a high content in vivo screen for modulators of developmental patterning in embryonic zebrafish, we previously identified eggmanone (EGM1, **3**) as a Hedgehog (Hh) signaling inhibitor functioning downstream of Smoothened. Phenotypic optimization studies for in vitro probe development utilizing a *Gli* transcription-linked stable luciferase reporter cell line identified EGM1 analogs with improved potency and aqueous solubility. Mechanistic profiling of optimized analogs indicated two distinct scaffold clusters: PDE4 inhibitors able to inhibit downstream of Sufu, and PDE4-independent Hh inhibitors functioning between Smo and Sufu. Each class represents valuable in vitro probes for elucidating the complex mechanisms of Hh regulation.

Published by Elsevier Ltd.

The Hedgehog (Hh) signaling pathway plays essential roles during animal development,[1] receiving extracellular signals in the form of the ligands Sonic Hedgehog (Shh) and to lesser extents Indian Hedgehog (Ihh) and Desert Hedgehog (Dhh) through the 12-pass transmembrane receptor Patched (Ptch). Ptch then relieves its inhibition of the 7-pass transmembrane G-protein coupled receptor Smoothened (Smo),[2,3] leading to Smo accumulation in the primary cilium and repression of the association between Suppressor of Fused (Sufu) and the Gli transcription factors (TF).[4] Translocation of Gli TFs to the nucleus then promotes transcription of Hh target genes; however, in the absence of extracellular ligands, Smo remains sequestered in cytoplasmic endosomes. Thus, the persistent Sufu-Gli complex in the primary cilium leads to proteasomal recognition and processing of Gli TFs to repressor forms, which upon nuclear translocation, inhibit Hh gene transcription.

Negative dysregulation or inhibition[5] of Hh signaling during development leads to holoprosencephaly and mis-specification of limbs, but in light of its control of cellular proliferation and differentiation, loss of function mutations in *Ptch1* (Gorlin syndrome) and *Sufu* and gain of function mutations in *Smo* and *Gli* are well annotated as oncogenic,[6–9] causing basal cell carcinoma (BCC),[10] medulloblastoma,[11,12] pancreatic cancer,[13] and other malignancies. Therefore, much effort focused primarily around small molecule antagonism of Smo yielded Vismodegib (GDC-0449, **1**)[14] as the first Hh-targeted therapy for the treatment of advanced BCC in 2012, thus validating the therapeutic hypothesis linking transcriptional inhibition and tumor burden reduction (Fig. 1). Subsequent FDA approval of Sonidegib (NVP-LDE225, **2**)[15] in 2015 led numerous other Smo antagonists in clinical development including PF-04449913,[16] IPI-926,[17] BMS-833923, TAK-441,[18] LY2940680, and itraconazole.[19] However, clinical experience with Smo antagonists[20] has revealed rapid and pervasive Smo antagonist-driven resistance and associated recurrence,[21–24] necessitating alternate strategies for Hh-driven cancer treatment.

We previously reported the discovery of eggmanone (EGM1, **3**)[25] from a high content screen for small molecule modulators of developmental patterning in embryonic zebrafish. Based on its recapitulation of the Hh-null phenotype, EGM1 was confirmed to inhibit Hh signaling in cell-based assays, functioning downstream of Smo and the negative regulator Sufu but upstream of Gli TFs. This downstream inhibition was linked to inhibition of phosphodiesterase 4 (PDE4) via protein kinase A (PKA) activation, leading to Gli phosphorylation and resultant Gli processing. Conceptual modulation of Hh transcriptional activity at signaling nodes downstream of Smo has gained favor for subverting clinical resistance,

* Corresponding author. Tel.: +1 615 936 7032; fax: +1 615 936 1872.
E-mail address: charles.c.hong@vanderbilt.edu (C.C. Hong).

http://dx.doi.org/10.1016/j.bmcl.2016.03.013
0960-894X/Published by Elsevier Ltd.

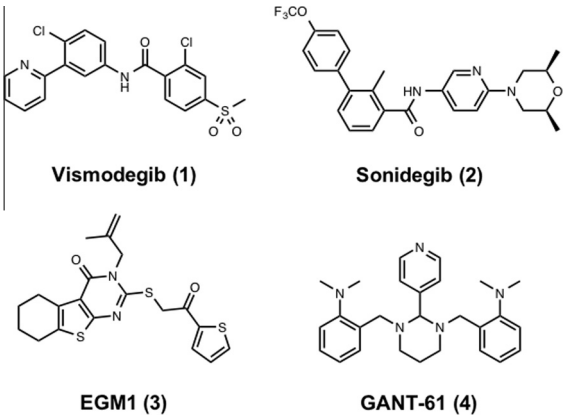

Figure 1. Structures of FDA-approved Smo antagonists (**1**, **2**), eggmanone (EGM1, **3**), and the Gli antagonist GANT-61 (**4**).

with Gli antagonism (GANT-61, **4**)[26] and bromodomain inhibition[27,28] emerging as two approaches. In addition to our studies with EGM1, mounting evidence has linked PDE4 to Hh signaling and tumorigenesis.[29,30] Therefore, we viewed EGM1 as a starting point for in vitro probe development toward an optimized downstream of Sufu Hh inhibitor; however, EGM1's limited aqueous solubility and modest potency required improvement.

We initially targeted three points of modification of EGM1: incorporation of polar atoms in the cyclohexyl ring, substitution of the methylallyl functionality, and replacement of the pendant thiophene. In linear fashion starting with cyclohexanone and derivatives (**5a**–**d**), the tricyclic ring system was fashioned from left to right starting with a Gewald reaction[31] to provide the 2-aminothiophene **6**. In most cases, formation of the dithiourea **7**[32] was followed by two-step cyclization with primary amines to yield the cyclic thiourea **8**; however, on smaller scales, direct formation of thioureas with isothiocyanates and subsequent cyclization also arrived at **8**.[33] *S*-alkylation under mild conditions installed alkyl ketones to provide EGM1 analogs **9a**–**n** and tetrahydropyran and tetrahydrothiopyran analogs **9o** and **9p**. In the case of Y = NBoc, further Boc deprotection gave piperidine **10a**.

When choosing our primary assay for analog evaluation, consideration was given to two factors: cellular reduction of Hh target gene *Gli1* transcription is directly linked to in vivo control of tumor growth,[10,12] and micromolar potency of the marketed PDE4 inhibitor Roflumilast for Hh signaling inhibition (data not shown) indicated partial contribution of PDE4 to EGM1's observed Hh inhibition. Therefore, we prioritized phenotypic analog evaluation in the *Gli*-responsive luciferase reporter line TM3-Gli-Luc[34] stimulated with 20 nM Smo agonist (SAG) while concurrently monitoring non-specific cellular toxicity. Additionally, lipophilic efficiency (LipE),[35] a concurrent readout of a compound's potency (pEC_{50}) and lipophilicity (*c*Log*P*) derived by subtracting the latter from the former, was utilized to optimize solubility properties (Table 1), allowing for straightforward tracking of compounds with improvements in both parameters. Marketed Smo antagonists Vismodegib and Sonidegib displayed expected potency, while the EC_{50} of the Gli antagonist GANT-61 was slightly higher than the reported ~5 μM EC_{50} in the Shh-LIGHT2 reporter line.[36] Pleased with the response of known Hh inhibitors, we profiled EGM1 and noted a benchmark EC_{50} for EGM1 of 1.34 μM and a corresponding LipE of 0.73. Given that the low-nanomolar EC_{50}s of **1** and **2** support LipEs of 4.33 and 3.02 respectively, we targeted a LipE for optimized EGM1 analogs of >2 deriving from an EC_{50} of <1 μM (pEC_{50} > 6). Replacement of the methylallyl group with small alkyl and cycloalkyl substituents revealed broad tolerance and a resulting improvement of LipE to 1.40 with cyclopropyl analog **9b**, driven by *c*Log*P* reduction. Phenyl analog **9f** indicated steric disfavoring of large substituents. In marked contrast to the favorable structure activity relationships (SAR) of the R^1 functionality, substitution of the R^2 thiophene in EGM1 showed little tolerance for alternate (hetero)aromatic and cycloalkyl amides with major potency losses across the series (**9g**–**n**). Only 2-methylpiperidine **9m** displayed an acceptable reduction in potency (~2-fold); however, an LD_{50} of 16.7 μM precluded further investigation. Therefore, bioisosteric replacement of the thiophene group for a phenyl ring was seen as a prudent strategy going forward despite the modest potency of **9g**. Finally, analogs **9o**, **9p**, and **10a** indicated disfavored incorporation of polar atoms into the western cyclohexyl ring.

Having established SAR for the most readily modifiable groups of EGM1, we next sought to explore replacements for the cyclohexylthiophene core, which we postulated could ameliorate inherent EGM1 solubility limitations. Therefore, we intercepted the Scheme 1 synthetic route with α-aminoarylesters, including benzothiophene **11** derived from three step conversion of 2-aminocyclohexylthiophene **6a** by a protection, oxidation, and deprotection strategy (Scheme 2). Benzothiophene **11** and readily available methyl anthranilate were converted to EGM1-like structures following Scheme 1 steps b–e, providing analogs **12** and **14a**–**c**.

Similar to analogs **14a**–**c**, in which we removed the cyclohexyl ring, arrival at the terminal thiophene core commenced by a modified Gewald reaction[37] with 1,4-dithiane-2,5-diol (**15**, Scheme 3). As in Scheme 1, conversion to dithiourea **17** was followed by two-step cyclization with primary amines to yield cyclic thioureas **18** which were *S*-alkylated to provide EGM1 analogs **19a**–**c**. In light of biological activity presented in Table 2, we further explored the role of the linker with **20a** and **20b** in which secondary and tertiary alcohols were formed from ketone **19c** by either reduction with $NaBH_4$ or Grignard addition with MeMgCl. Additionally, chloropyrimidinone **21** provided the necessary electrophilic center to investigate thioether modifications as the ether **22a** or secondary amine **22b** (Fig. 3).

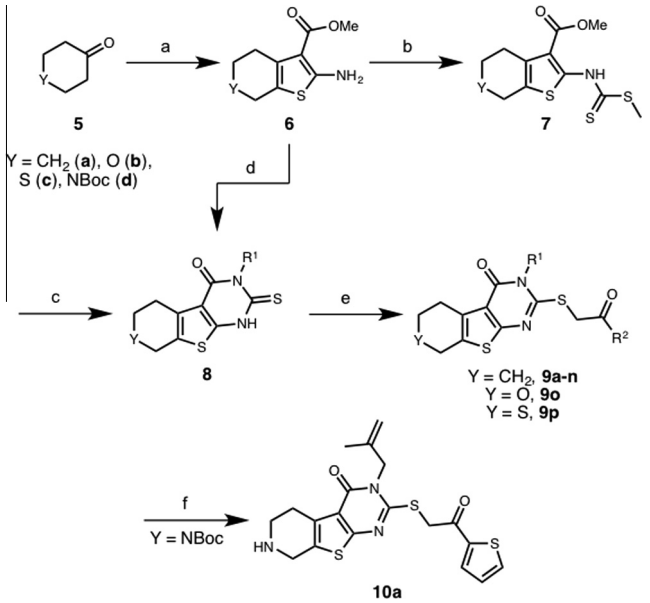

Scheme 1. Reagents and conditions: (a) S_8, $NCCH_2CO_2Me$, Et_3N, EtOH, rt, 16 h, 49–80%; (b) CS_2, NaOH, DMSO, H_2O, rt, 1 h then Me_2SO_4, rt, 3 h, 72–93%; (c) R^1NH_2, Et_3N, CH_3CN, 90 °C, 16 h; KOH, EtOH, H_2O, 70 °C, 4 h, 17–72%, two steps; (d) R^1NCS, PhMe, 115 °C, 72 h; KOH, EtOH, H_2O, 70 °C, 4 h, 16–80%, two steps; (e) $XCH_2C(O)R^2$, Cs_2CO_3, CH_3CN, rt, 3 h, 9–88%; (f) TFA, CH_2Cl_2, 0–25 °C, 3 h, 27%. X = Cl, Br.

Table 1
Initial EGM1 SAR with constant thienopyrimidinone core

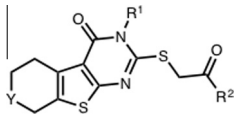

Entry	Y	R^1	R^2	TM3-Gli-Luc EC_{50}[a] (μM)	TM3-Gli-Luc LD_{50}[a] (μM)	LipE[b]
1	—	—	—	0.013 ± 0.004	>50	4.33
2	—	—	—	0.0012 ± 0.0002	>50	3.02
3	CH_2			1.34 ± 0.002	>50	0.73
4	—	—	—	9.27 ± 1.8	>50	1.34
9a	CH_2			2.36 ± 0.12	>50	1.03
9b	CH_2			1.89 ± 0.75	>50	1.40
9c	CH_2	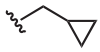		2.07 ± 0.87	>50	0.86
9d	CH_2	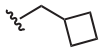		1.99 ± 1.1	45.6 ± 5.2	0.70
9e	CH_2			1.30 ± 0.18	>50	1.06
9f	CH_2	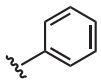		8.25 ± 0.14	>50	−0.15
9g	CH_2			5.70 ± 2.1	>50	−0.01
9h	CH_2			19.8 ± 1.0	>50	0.74
9i	CH_2			11.1 ± 0.59	35.4 ± 1.1	0.94
9j	CH_2			>20	>50	—
9k	CH_2			>20	>50	—
9l	CH_2			10.7 ± 1.4	24.6 ± 2.7	0.61
9m	CH_2			2.32 ± 0.73	16.7 ± 0.25	0.94
9n	CH_2			>20	>50	—
9o	O			>20	>50	—
9p	S			4.57 ± 1.8	>50	0.67
10a	NH			6.40 ± 0.33	20.1 ± 1.2	1.45

[a] Values represent mean ± standard error of the mean for at least two independent experiments performed in triplicate.
[b] Calculated as pEC_{50}—*c*Log*P*, determined by Molinspiration Cheminformatics.

The benzothiophene analog of EGM1 **12** displayed a complete loss of Hh inhibitory activity, likely due to disfavored conformational and/or aromatic effects compared to EGM1, and its physical properties precluded any further investigation of this scaffold (Table 2). Benzopyrimidinone **14a** similarly disappointed in its complete loss of activity; however, we were surprised to see that slight modifications to the eastern functionalities with **14b** and **14c** could more than return activity, yielding the first analogs with potency improvements over EGM1 and satisfying increases in LipE to above two. Even more promising was the thienopyrimidinone series **19a–c**, which met all of our initial qualifications of a quality in vitro Hh probe, where **19c** displayed exceptional potency and solubility with no non-specific cellular toxicity. Thus at this juncture, **19c** constituted our candidate in vitro Hh probe.

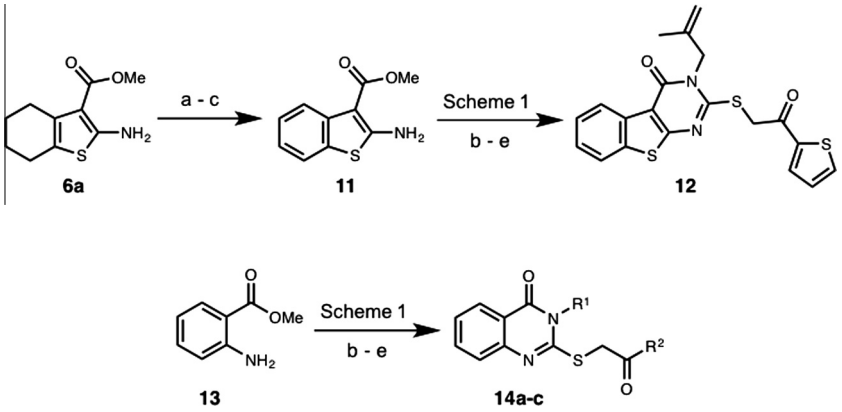

Scheme 2. Reagents and conditions: (a) AcCl, DMAP, THF, rt, 2 h, 82%; (b) DDQ, PhH, 85 °C, 5 d, 34%; (c) pyrrolidine, PhMe, 100 °C, 18 h, 87%.

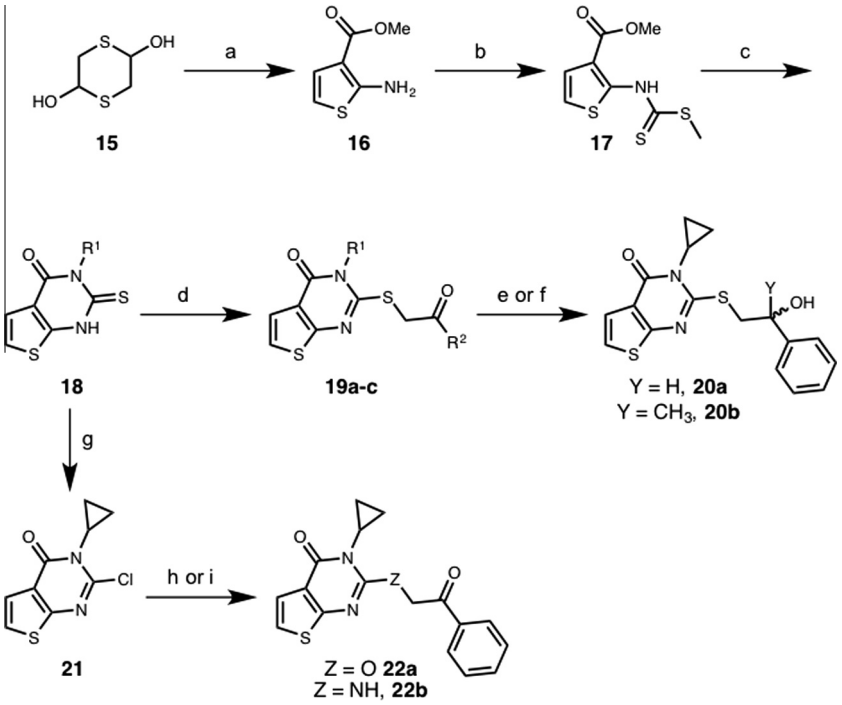

Scheme 3. Reagents and conditions: (a) $NCCH_2CO_2Me$, Et_3N, MeOH, DMF, 50 °C via μW, 3 min, 83%; (b) CS_2, NaOH, DMSO, H_2O, rt, 1 h then Me_2SO_4, rt, 3 h, 74%; (c) R^1NH_2, Et_3N, CH_3CN, 90 °C, 16 h; KOH, EtOH, H_2O, 70 °C, 4 h, 11–84%, two steps; (d) $XCH_2C(O)R^2$, Cs_2CO_3, CH_3CN, rt, 3 h, 21–71%; (e) $NaBH_4$, THF, EtOH, 0–25 °C, 2 h, 66%; (f) MeMgCl, THF, 0 °C, 1 h, 19%; (g) $POCl_3$, DMF, 0–55 °C, 72 h, 30%; (h) $PhC(O)CH_2OH$, NaH, THF, rt, 0.5 h, then **21**, 65 °C, 18 h, 1%; (i) $PhC(O)CH_2NH_2{\cdot}HCl$, DIPEA, *i*-PrOH, rt, 0.5 h, then **21**, 100 °C, 18 h, 8%. X = Cl, Br.

Our final SAR investigations focused on analog **19c** and the heretofore unexplored role of the thioether and attached linker (Fig. 2). Thus, secondary and tertiary alcohols **20a** and **20b** respectively indicated preference for the benzylic ketone moiety but showed only modest potency reductions, with **20a** still having a desirable probe profile with <500 nM potency and a LipE of 3.41. In contrast, the thioether proved essential to biological activity, with ether and secondary amine analogs **22a** and **22b** respectively showing complete loss of inhibition.

In light of EGM1's ability to halt Hh transcriptional activity at a node downstream of the negative regulator Sufu, and thus also downstream of Smo, we sought to confirm mode of action retention with our most promising analogs. Therefore, we employed *Sufu*$^{-/-}$ mouse embryonic fibroblasts (MEF)[38] that display constitutively active transcription of Hh target genes *Gli1* and *Ptch1* and monitored the ability of our optimized analogs to repress signaling via quantitative reverse transcription-PCR (qRT-PCR). Smo antagonists are expected to have no effect on the constitutively active signaling, and Sonidegib (**2**), tested at 0.1 μM (~100-fold its EC_{50}), failed to inhibit transcription of both genes (Table 3). In contrast, the Gli antagonist GANT-61 and EGM1 both showed significant reductions in transcription of *Gli1* and *Ptch1*, with approximately 50% inhibition at 10 μM. We then evaluated improved analogs from multiple structural classes including those from Table 1 with cyclohexylthiophene cores as well as from Table 2 with structurally distinct core modifications. Strikingly, while EGM1 analogs retaining the cyclohexyl-thiophene core (**9b**, **9e**, **9g**, **9m**) showed a general ability to inhibit transcriptional activity in the *Sufu*$^{-/-}$ cell line consistent with EGM1's mechanism of action, more potent TM3-Gli-Luc inhibitors lacking the western cyclohexyl ring (**14b**, **19b**, **19c**, **20a**) indicated a mechanistic drift, observed as a lack of *Sufu*$^{-/-}$ transcriptional inhibition. Specifically, **14b**, the most consistently potent inhibitor among the non-cyclohexyl group, showed 10% reduction of *Gli1* and *Ptch1* mRNA

Table 2
EGM1 analogs with core modifications

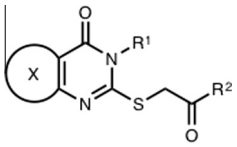

Entry	X	R^1	R^2	TM3-Gli-Luc EC_{50}[a] (μM)	TM3-Gli-Luc LD_{50}[a] (μM)	LipE[b]
12				>20	>50	—
14a				>20	>50	—
14b				0.685 ± 0.02	>50	2.78
14c				1.16 ± 0.39	>50	2.46
19a				0.931 ± 0.11	>50	2.06
19b				0.933 ± 0.10	>50	2.89
19c				0.082 ± 0.01	>50	3.84

[a] Values represent mean ± standard error of the mean for at least two independent experiments performed in triplicate.
[b] Calculated as pEC_{50}—*c*Log*P*, determined by Molinspiration Cheminformatics.

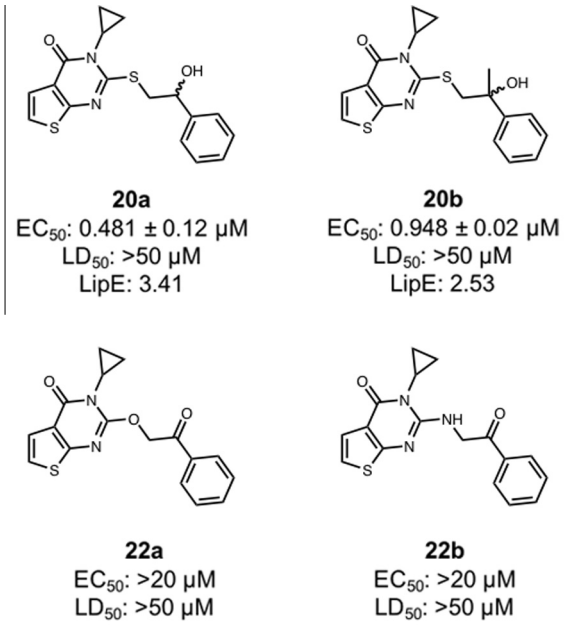

Figure 2. SAR of the linker functionality of **19c**.

transcripts at 10 μM; however, with a TM3-Gli-Luc EC_{50} of 0.685 μM, these results indicate that **14b** and structurally related non-cyclohexylthiophene analogs function at a node upstream of Sufu.

Multiple factors may be responsible for the divergence of EGM1 analogs' efficacy in the *Sufu*$^{-/-}$ cell line; therefore, we profiled select analogs in a set of assays devised to illuminate their mechanistic underpinnings. First, we revisited the contribution of PDE4 as a potential explanation for the observed mechanistic drift.

Table 3
Summary of optimized analogs and mechanistic profiling

Entry	TM3-Gli-Luc EC_{50} (μM)	LipE	*Sufu*$^{-/-}$ % Inh. *Gli1* mRNA[a,b]	*Sufu*$^{-/-}$ % Inh. *Ptch1* mRNA[a,b]	PDE4D IC_{50}[a] (μM)
2	0.0012 ± 0.0002	3.02	5.8 ± 4.0	−0.2 ± 2.1	—
3	1.34 ± 0.002	0.73	46.5 ± 5.1	32.2 ± 1.9	0.380 ± 0.02
4	9.27 ± 1.8	1.34	43.8 ± 5.2	52.8 ± 2.7	—
9b	1.89 ± 0.75	1.40	26.8 ± 8.4	26.5 ± 1.1	N/D
9e	1.30 ± 0.18	1.06	44.9 ± 5.1	39.9 ± 6.6	0.486 ± 0.001
9g	5.70 ± 2.1	−0.01	64.8 ± 0.65	60.4 ± 1.9	0.965 ± 0.10
9m	2.32 ± 0.73	0.94	35.0 ± 2.1	49.2 ± 1.8	N/D
14b	0.685 ± 0.02	2.78	10.3 ± 4.8	9.9 ± 5.6	N/D
19b	0.933 ± 0.10	2.89	5.5 ± 4.4	−3.3 ± 2.2	N/D
19c	0.082 ± 0.01	3.84	13.6 ± 2.6	−0.3 ± 4.5	3.10 ± 0.48
20a	0.481 ± 0.12	3.41	3.2 ± 2.2	−4.8 ± 3.3	6.07 ± 1.5

N/D = not determined.
[a] Values represent mean ± standard error of the mean for at least two independent experiments performed in triplicate normalized to DMSO.
[b] Compounds tested at 10 μM, except Sonidegib tested at 0.1 μM.

Against the consensus PDE4D sequence, EGM1 displayed an IC_{50} of 0.380 μM, slightly less potent than previously reported but likely due to minor isoform variation. Related cyclohexylthiophene analogs **9e** and **9g** tracked well with EGM1's IC_{50}:EC_{50} ratio; however, interestingly the potent Hh inhibitors **19c** and **20a** showed only modest IC_{50}s against PDE4D. These results indicate that the ability of cyclohexylthiophene analogs to function downstream of Sufu is dependent on their ability to inhibit PDE4, and that the observed mechanistic drift of non-cyclohexylthiophene analogs results from a decreased ability to inhibit PDE4.

Next, considering the mechanistic drift of robotnikinin analogs to Smo antagonists,[39] we evaluated **14b**, **19b**, **19c**, and **20a** in a competition assay for the Smo cyclopamine (Cyc) binding site to determine if the Hh potency of non-cyclohexylthiophene analogs could be explained by Smo antagonism (Fig. 3). Thus, HEK-293T

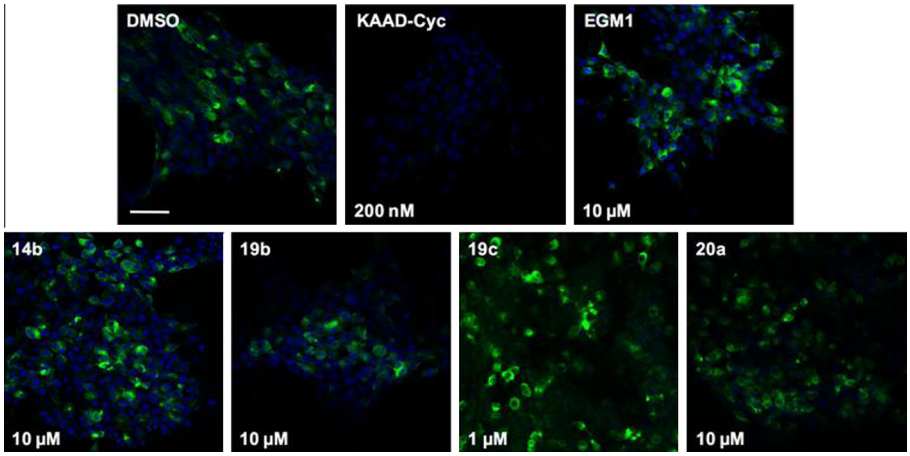

Figure 3. EGM1 analogs lacking activity downstream of Sufu do not displace the binding of BODIPY-cyclopamine (5 nM) from its Smo binding site at the indicated concentrations, in contrast to KAAD-cyclopamine (200 nM). Green = BODIPY-cyclopamine; blue = DAPI. Scale bar = 20 μm.

cells overexpressing Smo were concurrently treated with 5 nM BODIPY-Cyc and molecules of interest. The potent Smo antagonist KAAD-Cyc completely displaced BODIPY-Cyc at 200 nM, and EGM1, as previously reported, showed no ability to compete for Smo binding. At the indicated concentrations (10- to 20-fold their EC_{50}s), non-cyclohexylthiophene analogs **14b**, **19b**, **19c**, and **20a** failed to compete for the Smo binding site, indicating that their functional target lay in between Smo and Sufu. Finally, EGM1 and analogs from Table 3 do not inhibit luciferase, as tested in a BMP-responsive element stable reporter cell line (data not shown).

Phenotypic screening and subsequent development allows for relevant clinical mechanism-driven discovery and optimization as well as novel target elucidation for improved targeted therapy strategies. Using this phenotypic optimization strategy, we have identified small molecule Hh inhibitors based on the EGM1 scaffold. As EGM1 functions downstream of the most targeted node within the pathway which is also commonly associated with clinical resistance, we expected analogs to retain this activity. Removal of the western-most cyclohexyl ring provided analogs with significant TM3-Gli-Luc potency and solubility improvements, with **19c** constituting our most promising compound. This analog series, in contrast to EGM1 and cyclohexylthiophene analogs, displayed an inability to inhibit constitutively active signaling at or downstream of Sufu, which was correlated with reduced PDE4 inhibition; interestingly, these compounds do not directly target Smo. Finally, cyclohexylthiophene analogs **9b** and **9e**, which retain the ability to inhibit both PDE4 and Hh signaling downstream of Sufu, constitute EGM1 analogs with improved aqueous solubility.

In summary, our results indicate that non-cyclohexylthiophene analogs inhibit Hh signaling via a PDE4-independent mechanism which functions in between Smo and Sufu, whereas cyclohexylthiophene analogs inhibit Hh signaling via a PDE4-dependent mechanism downstream of Sufu. It is thus notable that this PDE4-independent activity leading to significant improvements in Hh inhibition potency would have not been discovered using a target-based optimization approach. While we do not have direct evidence, it seems reasonable to hypothesize that the parent compound EGM1 and cyclohexylthiophene analogs display dual PDE4-dependent and PDE4-independent mechanisms of action rather than that non-cyclohexylthiophene analogs gained a new functionality not present in EGM1. Compounds from both series are valuable in vitro probes, as neither compete for Smo binding, and thus will be further utilized to elucidate the complex mechanisms of Hh signal regulation toward future targeted Hh therapeutics.

Acknowledgments

We thank Sarah Luchansky and Novartis Institutes for BioMedical Research for the TM3-Gli-Luc cell line. We thank Gary Sulikowski and Shaun Stauffer for helpful discussions, feedback, and support for synthesis. Confocal microscopy was performed in part through the use of the VUMC Cell Imaging Shared Resource (supported by United States NIH grants CA68485, DK20593, DK58404, DK59637 and EY08126). J.E.H. is supported by an American Heart Association Postdoctoral Fellowship (14POST19550002), and C.C.H. is supported by United States NIH R01HL104040 and La Jolla Pharmaceuticals.

Supplementary data

Supplementary data (synthetic procedures for **9b**, **9e**, **9g**, **9m**, **14b**, **19b**, **19c**, and **20a**, as well as bioassay protocols) associated with this article can be found, in the online version, at http://dx.doi.org/10.1016/j.bmcl.2016.03.013.

References and notes

1. Ryan, K. E.; Chiang, C. *J. Biol. Chem.* **2012**, *287*, 17905.
2. Taipale, J.; Cooper, M. K.; Maiti, T.; Beachy, P. A. *Nature* **2002**, *418*, 892.
3. Sharpe, H. J.; Wang, W.; Hannoush, R. N.; de Sauvage, F. J. *Nat. Chem. Biol.* **2015**, *11*, 246.
4. Hui, C.-C.; Angers, S. *Annu. Rev. Cell Dev. Biol.* **2011**, *27*, 513.
5. Chen, J. K.; Taipale, J.; Cooper, M. K.; Beachy, P. A. *Genes Dev.* **2002**, *16*, 2743.
6. Ng, J. M. Y.; Curran, T. *Nat. Rev. Cancer* **2011**, *11*, 493.
7. Kar, S.; Deb, M.; Sengupta, D.; Shilpi, A.; Bhutia, S. K.; Patra, S. K. *Exp. Cell Res.* **2012**, *318*, 1959.
8. Kasper, M.; Regl, G.; Frischauf, A.-M.; Aberger, F. *Eur. J. Cancer* **2006**, *42*, 437.
9. Mahindroo, N.; Punchihewa, C.; Fujii, N. *J. Med. Chem.* **2009**, *52*, 3829.
10. Hoff; Von, D. D.; LoRusso, P. M.; Rudin, C. M.; Reddy, J. C.; Yauch, R. L.; Tibes, R.; Weiss, G. J.; Borad, M. J.; Hann, C. L.; Brahmer, J. R.; Mackey, H. M.; Lum, B. L.; Darbonne, W. C.; Marsters, J. C., Jr.; de Sauvage, F. J.; Low, J. A. *N. Eng. J. Med.* **2009**, *361*, 1164.
11. Berman, D. M.; Karhadkar, S. S.; Hallahan, A. R.; Pritchard, J. I.; Eberhart, C. G.; Watkins, D. N.; Chen, J. K.; Cooper, M. K.; Taipale, J.; Olson, J. M.; Beachy, P. A. *Science* **2002**, *297*, 1559.
12. Rudin, C. M.; Hann, C. L.; Laterra, J.; Yauch, R. L.; Callahan, C. A.; Fu, L.; Holcomb, T.; Stinson, J.; Gould, S. E.; Coleman, B.; LoRusso, P. M.; Hoff; Von, D. D.; de Sauvage, F. J.; Low, J. A. *N. Eng. J. Med.* **2009**, *361*, 1173.
13. Rosow, D. E.; Liss, A. S.; Strobel, O.; Fritz, S.; Bausch, D.; Valsangkar, N. P.; Alsina, J.; Kulemann, B.; Park, J. K.; Yamaguchi, J.; LaFemina, J.; Thayer, S. P. *Surgery* **2012**, *152*, S19.
14. Robarge, K. D.; Brunton, S. A.; Castanedo, G. M.; Cui, Y.; Dina, M. S.; Goldsmith, R.; Gould, S. E.; Guichert, O.; Gunzner, J. L.; Halladay, J.; Jia, W.; Khojasteh, C.; Koehler, M. F. T.; Kotkow, K.; La, H.; LaLonde, R. L.; Lau, K.; Lee, L.; Marshall, D.; Marsters, J. C., Jr.; Murray, L. J.; Qian, C.; Rubin, L. L.; Salphati, L.; Stanley, M. S.; Stibbard, J. H. A.; Sutherlin, D. P.; Ubhayaker, S.; Wang, S.; Wong, S.; Xie, M. *Bioorg. Med. Chem. Lett.* **2009**, *19*, 5576.

15. Pan, S.; Wu, X.; Jiang, J.; Gao, W.; Wan, Y.; Cheng, D.; Han, D.; Liu, J.; Englund, N. P.; Wang, Y.; Peukert, S.; Miller-Moslin, K.; Yuan, J.; Guo, R.; Matsumoto, M.; Vattay, A.; Jiang, Y.; Tsao, J.; Sun, F.; Pferdekamper, A. C.; Dodd, S.; Tuntland, T.; Maniara, W.; Kelleher, J. F.; Yao, Y.-M.; Warmuth, M.; Williams, J.; Dorsch, M. *ACS Med. Chem. Lett.* **2010**, *1*, 130.
16. Munchhof, M. J.; Li, Q.; Shavnya, A.; Borzillo, G. V.; Boyden, T. L.; Jones, C. S.; LaGreca, S. D.; Martinez-Alsina, L.; Patel, N.; Pelletier, K.; Reiter, L. A.; Robbins, M. D.; Tkalcevic, G. T. *ACS Med. Chem. Lett.* **2012**, *3*, 106.
17. Tremblay, M. R.; Lescarbeau, A.; Grogan, M. J.; Tan, E.; Lin, G.; Austad, B. C.; Yu, L.-C.; Behnke, M. L.; Nair, S. J.; Hagel, M.; White, K.; Conley, J.; Manna, J. D.; Alvarez-Diez, T. M.; Hoyt, J.; Woodward, C. N.; Sydor, J. R.; Pink, M.; MacDougall, J.; Campbell, M. J.; Cushing, J.; Ferguson, J.; Curtis, M. S.; McGovern, K.; Read, M. A.; Palombella, V. J.; Adams, J.; Castro, A. C. *J. Med. Chem.* **2009**, *52*, 4400.
18. Ohashi, T.; Oguro, Y.; Tanaka, T.; Shiokawa, Z.; Tanaka, Y.; Shibata, S.; Sato, Y.; Yamakawa, H.; Hattori, H.; Yamamoto, Y.; Kondo, S.; Miyamoto, M.; Nishihara, M.; Ishimura, Y.; Tojo, H.; Baba, A.; Sasaki, S. *Bioorg. Med. Chem.* **2012**, *20*, 5507.
19. Kim, J.; Aftab, B. T.; Tang, J. Y.; Kim, D.; Lee, A. H.; Rezaee, M.; Kim, J.; Chen, B.; King, E. M.; Borodovsky, A.; Riggins, G. J.; Epstein, E. H.; Beachy, P. A.; Rudin, C. M. *Cancer Cell* **2013**, *23*, 23.
20. Low, J. A.; de Sauvage, F. J. *J. Clin. Oncol.* **2010**, *28*, 5321.
21. Metcalfe, C.; de Sauvage, F. J. *Cancer Res.* **2011**, *71*, 5057.
22. Atwood, S. X.; Sarin, K. Y.; Whitson, R. J.; Li, J. R.; Kim, G.; Rezaee, M.; Ally, M. S.; Kim, J.; Yao, C.; Chang, A. L. S.; Oro, A. E.; Tang, J. Y. *Cancer Cell* **2015**, *27*, 342.
23. Sharpe, H. J.; Pau, G.; Dijkgraaf, G. J.; Basset-Seguin, N.; Modrusan, Z.; Januario, T.; Tsui, V.; Durham, A. B.; Dlugosz, A. A.; Haverty, P. M.; Bourgon, R.; Tang, J. Y.; Sarin, K. Y.; Dirix, L.; Fisher, D. C.; Rudin, C. M.; Sofen, H.; Migden, M. R.; Yauch, R. L.; de Sauvage, F. J. *Cancer Cell* **2015**, *27*, 327.
24. Yauch, R. L.; Dijkgraaf, G. J. P.; Alicke, B.; Januario, T.; Ahn, C. P.; Holcomb, T.; Pujara, K.; Stinson, J.; Callahan, C. A.; Tang, T.; Bazan, J. F.; Kan, Z.; Seshagiri, S.; Hann, C. L.; Gould, S. E.; Low, J. A.; Rudin, C. M.; de Sauvage, F. J. *Science* **2009**, *326*, 572.
25. Williams, C. H.; Hempel, J. E.; Hao, J.; Frist, A. Y.; Williams, M. M.; Fleming, J. T.; Sulikowski, G. A.; Cooper, M. K.; Chiang, C.; Hong, C. C. *Cell Rep.* **2015**, *11*, 43.
26. Infante, P.; Alfonsi, R.; Botta, B.; Mori, M.; Di Marcotullio, L. *Trends Pharmacol. Sci.* **2015**, *36*, 547.
27. Tang, Y.; Gholamin, S.; Schubert, S.; Willardson, M. I.; Lee, A.; Bandopadhayay, P.; Bergthold, G.; Masoud, S.; Nguyen, B.; Vue, N.; Balansay, B.; Yu, F.; Oh, S.; Woo, P.; Chen, S.; Ponnuswami, A.; Monje, M.; Atwood, S. X.; Whitson, R. J.; Mitra, S.; Cheshier, S. H.; Qi, J.; Beroukhim, R.; Tang, J. Y.; Wechsler-Reya, R.; Oro, A. E.; Link, B. A.; Bradner, J. E.; Cho, Y.-J. *Nat. Med.* **2014**, *20*, 732.
28. Long, J.; Li, B.; Rodriguez-Blanco, J.; Pastori, C.; Volmar, C.-H.; Wahlestedt, C.; Capobianco, A.; Bai, F.; Pei, X.-H.; Ayad, N. G.; Robbins, D. J. *J. Biol. Chem.* **2014**, *289*, 35494.
29. Powers, G. L.; Hammer, K. D. P.; Domenech, M.; Frantskevich, K.; Malinowski, R. L.; Bushman, W.; Beebe, D. J.; Marker, P. C. *Mol. Cancer Res.* **2015**, *13*, 149.
30. Ge, X.; Milenkovic, L.; Suyama, K.; Hartl, T.; Purzner, T.; Winans, A.; Meyer, T.; Scott, M. P. *eLife Sci.* **2015**, *4*, e07068.
31. Fondjo, E. S.; Döpp, D.; Henkel, G. *Tetrahedron* **2006**, *62*, 7121.
32. Alagarsamy, V.; Rajesh, R.; Ramaseshu, M.; Vijaykumar, S.; Ramseshu, K. V.; Duraianandakumar, T. *Biol. Pharm. Bull.* **2004**, *27*, 652.
33. Ivachtchenko, A.; Kovalenko, S.; Tkachenko, O. V.; Parkhomenko, O. *J. Comb. Chem.* **2004**, *6*, 573.
34. Miller-Moslin, K.; Peukert, S.; Jain, R. K.; McEwan, M. A.; Karki, R.; Llamas, L.; Yusuff, N.; He, F.; Li, Y.; Sun, Y.; Dai, M.; Perez, L.; Michael, W.; Sheng, T.; Lei, H.; Zhang, R.; Williams, J.; Bourret, A.; Ramamurthy, A.; Yuan, J.; Guo, R.; Matsumoto, M.; Vattay, A.; Maniara, W.; Amaral, A.; Dorsch, M.; Kelleher, J. F. *J. Med. Chem.* **2009**, *52*, 3954.
35. Shultz, M. D. *Bioorg. Med. Chem. Lett.* **2013**, *23*, 5980.
36. Lauth, M.; Bergström, A.; Shimokawa, T.; Toftgård, R. *Proc. Natl. Acad. Sci. U.S.A.* **2007**, *104*, 8455.
37. Hesse, S.; Perspicace, E.; Kirsch, G. *Tetrahedron Lett.* **2007**, *48*, 5261.
38. Svärd, J.; Heby-Henricson, K.; Henricson, K. H.; Persson-Lek, M.; Rozell, B.; Lauth, M.; Bergström, A.; Ericson, J.; Toftgård, R.; Teglund, S. *Dev. Cell* **2006**, *10*, 187.
39. Dockendorff, C.; Nagiec, M. M.; Weïwer, M.; Buhrlage, S.; Ting, A.; Nag, P. P.; Germain, A.; Kim, H.-J.; Youngsaye, W.; Scherer, C.; Bennion, M.; Xue, L.; Stanton, B. Z.; Lewis, T. A.; MacPherson, L.; Palmer, M.; Foley, M. A.; Perez, J. R.; Schreiber, S. L. *ACS Med. Chem. Lett.* **2012**, *3*, 808.